Volume 61
Number 3
11 January 2025
Pages 379–586

ChemComm

Chemical Communications

rsc.li/chemcomm

ISSN 1359-7345

ROYAL SOCIETY OF CHEMISTRY

COMMUNICATION

Tsuyoshi Minami *et al.*

Colorimetric quantitative detection of steroid hormones using an indicator displacement assay-based chemosensor array

ChemComm

COMMUNICATION

View Article Online
View Journal | View Issue

Cite this: *Chem. Commun.*, 2025, **61**, 476

Received 6th November 2024,
Accepted 25th November 2024

DOI: 10.1039/d4cc05791k

rsc.li/chemcomm

Colorimetric quantitative detection of steroid hormones using an indicator displacement assay-based chemosensor array†

Yui Sasaki, [abc] Yusuke Yamanashi,[d] Kohei Ohshiro, [b] Xiaojun Lyu [b] and Tsuyoshi Minami *[b]

A colorimetric chemosensor array based on an indicator displacement assay has achieved not only visualization of differences in hormone structures but also quantitative detection of sex hormones in their mixtures. Furthermore, the chemosensor array has allowed the detection of a steroid hormone in diluted human saliva.

Steroid hormones are essential biomarkers playing significant roles such as sexual functions in the human body.[1] For example, testosterone (H2) is the representative sex hormone related to the health status of men.[1b] Testosterone is converted into 17β-estradiol (H7) by aromatase.[1c] The levels of both testosterone and 17β-estradiol involve sexual functions and their disease.[1] In addition, dehydroepiandrosterone (H5), 17β-estradiol (H7), and progesterone (H13) are salivary markers to examine burning mouth syndrome.[1d] Therefore, the qualitative and quantitative detection approaches are important for the practical analysis of steroid hormones. Among macrocyclic hosts,[2] cucurbit[*n*]urils (CB[*n*]) with hydrophobic inside cavities are capable of encapsulating not only hydrophobic (*e.g.*, testosterone (H2) and progesterone (H13)) but also cationic steroids (*e.g.*, pancuronium bromide (H11) and vecuronium bromide (H15)).[3] Moreover, the hydrophilic portals made of ureidyl C=O moieties can be used to recognize the binding sites of analytes through non-covalent interactions (*e.g.*, hydrogen bonds), which contribute to distinguishing analyte geometries with structural similarities.[3,4] Considering the geometries of target steroid hormones (H1–H15), cucurbit[8]uril (CB[8]) was used as a macrocyclic receptor in this assay. Compared with CB[7], the larger cavity size is superior to the encapsulation of hydrophobic steroid hormones depending on their size and structure geometry.[3d]

Chemosensors comprising indicator and receptor units are potent analytical tools to visualize molecular recognition information.[5] Based on inherent cross-reactivities of artificial receptors, chemosensors can bind to various analytes with similar structures through intermolecular interactions.[6] Such chemosensors show cross-reactive optical responses depending on the types of analytes and their concentrations, which allow simultaneous discrimination based on pattern recognition.[6] Herein, indicator displacement assay (IDA)-based chemosensors were employed to detect various steroid hormones simultaneously based on pattern recognition. Although macrocyclic-type chemosensors including CB[*n*] have been vigorously developed for the detection of steroid hormones in supramolecular chemistry fields,[2,3] simultaneous discrimination has not been achieved yet. The difficulty of the quantitative assay is attributed to non-linear sensor responses in analyte mixtures or the presence of interferents. Herein, we propose a colorimetric chemosensor array system combined with pattern recognition methods for simultaneous and quantitative discrimination of steroid hormones. In this study, 4-(*N*,*N*′-dimethylamino)-azobenzene derivatives (*i.e.*, X = $-NH_2$ (**1**), –OH (**2**)) and a 4-phenylazopyridine derivative (**3**) were selected as indicators to achieve colorimetric detection (Fig. 1). A transformation of the indicators (**1** and **2**) to azonium structures causes drastic color changes,[7] which is induced by CB[*n*] encapsulation.[3d] In addition, the 4-phenylazopyridine derivative (**3**) shows unique optical properties because of a pyridine unit as a proton acceptor.[8]

The complexation based on displacement among an indicator (*i.e.*, **2**), CB[8], and a steroid hormone (*i.e.*, testosterone) was evaluated by ^{1}H NMR and MS analyses. Considering the solubility of the indicator and CB[8], and optical properties according to azonium formation,[3d,7,8] all measurements were carried out in an aqueous DMSO solution (DMSO : water = 1 : 9, v/v) at pH 3.2 at 25 °C. Fig. S1(a) and (b), ESI† show upfield shifts in aryl proton peaks of **2** upon the addition of CB[8]. In particular, the chemical

[a] *Research Center for Advanced Science and Technology, The University of Tokyo, 4-6-1, Komaba, Meguro-ku, Tokyo, 153-8904, Japan*
[b] *Institute of Industrial Science, The University of Tokyo, 4-6-1 Komaba, Meguro-ku, Tokyo, 153-8505, Japan. E-mail: tminami@g.ecc.u-tokyo.ac.jp*
[c] *JST, PRESTO, 4-1-8 Honcho, Kawaguchi, Saitama, 332-0012, Japan*
[d] *JNC Petrochemical Corp., 5-1, Goikaigan, Ichihara, Chiba, Japan*

† Electronic supplementary information (ESI) available: Regents and materials, apparatuses and methods, ^{1}H NMR analysis, DFT calculations, UV-vis titrations, estimation of association constants, array experiments. See DOI: https://doi.org/10.1039/d4cc05791k

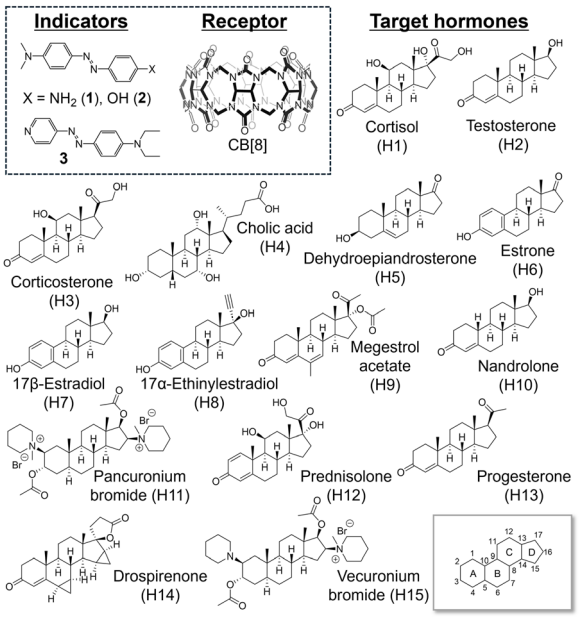

Fig. 1 Chemical structures of indicators (**1–3**), a receptor (CB[8]), and target steroid hormones (H1–H15) for an indicator-displacement assay-based colorimetric detection.

shifts of aryl protons of **2** marked with a red circle and a purple square indicated that the 4-(*N*,*N*′-dimethylamino)benzene unit was encapsulated by CB[8] (Fig. S1(b), ESI†).[3d] In addition, the DFT calculation result for the complexation of **2** and CB[8] suggested the encapsulation of the 4-(*N*,*N*′-dimethylamino) benzene unit (Fig. S3, ESI†). Meanwhile, a pattern of the aryl proton peaks of **2** in the presence of CB[8] and testosterone (Fig. S1(c), ESI†) showed a similar to that of the indicator only (Fig. S1(a), ESI†). The return back of the chemical shifts indicated the removal of **2** from the complex of **2**·CB[8] upon the addition of testosterone.[3d] Furthermore, MS analysis results supported 1 to 1 binding stoichiometric complexations of **2**·CB[8] (Fig. S5(a)) and CB[8] and testosterone (Fig. S5(b)), ESI,† respectively. These analyses supported the displacement assay among the indicator, CB[8], and the steroid hormone.

Next, colorimetric responses derived from the complexation between the indicators and CB[8] were evaluated by UV-vis host titrations. The absorption bands of **1** and **2** showed redshifts upon the addition of CB[8], which suggested an increase in the number of azonium forms (Fig. S6 and S7, ESI†).[7] Indeed, DFT calculation results for the complexations of **1** or **2** and CB[8] revealed a hydrogen bond between an N–H bond of the indicator and an ureidyl C=O moiety of CB[8] (Fig. S2 and S3, ESI†).[3d] Meanwhile, the 4-phenylazopyridine derivative (**3**) responded to CB[8] accompanied by blueshifts (Fig. S8, ESI†), which can be explained by the role of the pyridine unit as a proton acceptor.[8] Moreover, the DFT calculation result suggested the encapsulation of **3** by CB[8] (Fig. S4, ESI†). The binding affinities based on the UV-vis titration isotherms were estimated to be $(3.7 \pm 0.6) \times 10^5$ M^{-1} for **1**, $(9.0 \pm 2.1) \times 10^5$ M^{-1} for **2**, and $(4.7 \pm 0.55) \times 10^5$ M^{-1} for **3**, respectively.

Subsequently, the detection ability of the IDA-based chemosensors (*i.e.*, **1**·CB[8], **2**·CB[8], and **3**·CB[8]) was assessed for 15 types of target steroid hormones. The evaluated target steroid hormones are categorized based on their structural geometries, such as cyclohex-2-en-1-one structures at ring A with methyl groups at carbon 10 positions, cationic skeletons, cyclohexanol, and phenol structures (Fig. 1). Fig. 2 shows examples of UV-vis titration profiles of **2**·CB[8] for testosterone (H2) and **3**·CB[8] for progesterone (H13), respectively. According to the difference in optical properties in the presence of CB[8], the different color changes between **2**·CB[8] and **3**·CB[8] were observed upon analyte addition (Fig. 3, inset). Among the target steroid hormones, testosterone (H2), progesterone (H13), and drospirenone (H14) induced drastic color changes, which showed higher binding affinities to the chemosensors (Table S1, ESI†). These steroid hormones possess common cyclohex-2-en-1-one structures at ring A with methyl groups at carbon 10 positions. The methyl substitution allows the depth immersion of the hydrophobic analytes into the CB[8] cavity.[3d] In this regard, three chemosensors showed different binding affinities between testosterone (H2) and nandrolone (H10) because of differences in the absence or presence of a methyl group at the carbon 10 position. However, binding affinities for cortisol (H1) and corticosterone (H3) were moderate even in the same backbone. The difference in the binding affinities might be explained by the increase in hydrophilicity of steroid skeletons owing to substitution groups such as hydroxy and carboxy groups.[3d] Moreover, the inherent nature of CB[8] allowed drastic colorimetric changes against cationic analytes such as pancuronium bromide (H11) and vecuronium bromide (H15).[3c,d] Meanwhile, weak and/or moderate responses were observed by adding cyclohexanol (*i.e.*, cholic acid (H4)) and

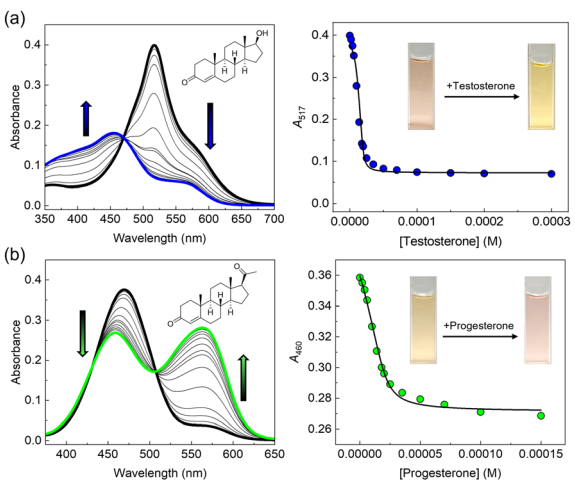

Fig. 2 UV-vis absorption spectra of the complex of indicator (10 μM) and CB[8] (20 μM) upon the addition of target steroid hormones in an aqueous DMSO solution (DMSO : water = 1 : 9, v/v) at pH 3.2 at 25 °C. (a) **2** for testosterone and (b) **3** for progesterone. The titration isotherms were obtained by collecting the maximum absorbance at 517 nm for **2** and 460 nm for **3**. Insets show color changes in chemosensors before and after adding (a) testosterone (300 μM) and (b) progesterone (150 μM), respectively. [Indicator] = 10 μM, [CB[8]] = 20 μM.

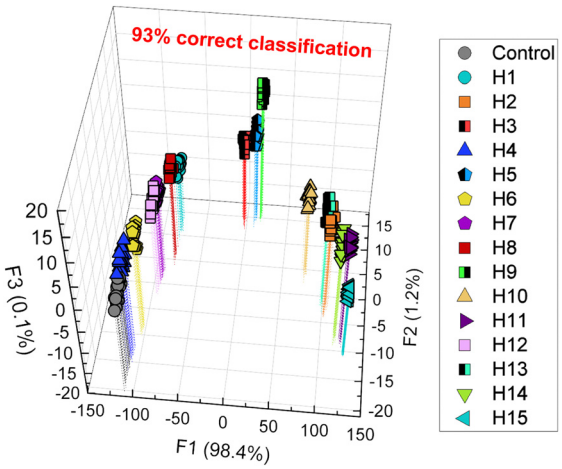

Fig. 3 Qualitative assay for 15 steroid hormones using LDA. The inset data contained UV-vis absorption spectra of three chemosensors (**1**·CB[8], **2**·CB[8], and **3**·CB[8]) before and after adding steroid hormones. [Indicator] = 10 μM, [CB[8]] = 20 μM, and [steroid hormone] = 30 μM. Control means cluster in the absence of analytes.

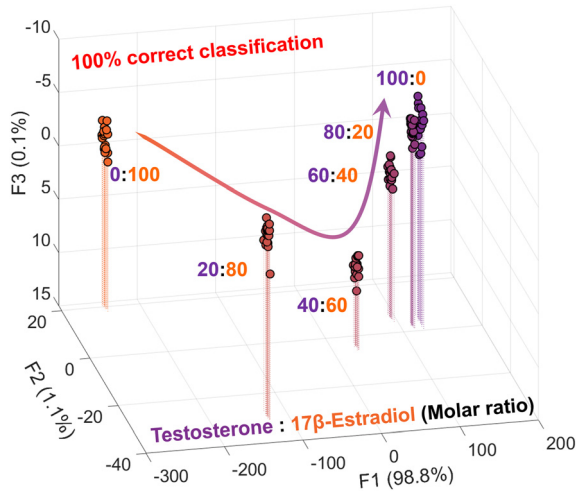

Fig. 4 Semi-quantitative assay using LDA for simultaneous discrimination of testosterone (H2) and 17β-estradiol (H7) in their mixtures at different molar ratios. The inset data contained UV-vis absorption spectra of three chemosensors (**1**·CB[8], **2**·CB[8], and **3**·CB[8]) in the presence of mixtures of steroid hormones. The total concentration for analyte mixtures was set as 25 μM. [Indicator] = 10 μM, [CB[8]] = 20 μM.

phenol structures (*i.e.*, estrone (H6), 17β-estradiol (H7), 17α-ethinyl estradiol (H8), and prednisolone (H12)). Although dehydroepiandrosterone (H5) is classified into cyclohexanol, obvious color changes were observed because of the methyl group at the carbon 10 position. Indeed, three chemosensors showed cross-reactive responses for 15 analytes depending on differences in their chemical structures and properties, which provided various orders of association constants (Table S1, ESI†). Thus, the differences in molecular geometries and hydrophobicity of analytes are significant factors in discriminating analyte structures based on pattern recognition. The limit of detection of each chemosensor was estimated based on the 3σ method (Table S2, ESI†).[9]

As the next attempt, a qualitative assay was carried out to reveal the potential of the colorimetric chemosensors for the discrimination of 15 analytes. A data matrix was constructed by UV-vis absorption spectra of three chemosensors before and after adding the target steroid hormones at 30 μM. The obtained inset data contained multidimensional information corresponding to three chemosensors, 15 analytes, and 20 repetitions for each validation. Therefore, linear discriminant analysis (LDA) was employed to decrease the dimension of the inset data and classify each component based on their differences.[10] As shown in Fig. 3, 16 clusters including control and 15 analytes were distributed with a 93% correct classification rate. Notably, the cluster distribution almost depended on the order of the binding affinities. In particular, the clusters on the right side of factor 1 (F1) were categorized based on cyclohex-2-en-1-one structures at ring A with methyl groups at carbon 10 positions (*i.e.*, testosterone (H2), progesterone (H13), and drospirenone (H14)) and cationic skeletons (*i.e.*, pancuronium bromide (H11) and vecuronium bromide (H15)). Moreover, the position of clusters of cortisol (H1) and corticosterone (H3) indicated lower binding affinities than the above-mentioned analytes. Moreover, the clusters on the left side of F1 included cyclohexanol (*i.e.*, cholic acid (H4) and dehydroepiandrosterone (H5)) and phenol structures (*i.e.*, estrone (H6), 17β-estradiol (H7), 17α-ethinylestradiol (H8), and prednisolone (H12)).

In the qualitative assay, the chemosensor array achieved the categorization of analyte structures based on the difference in the skeletons of ring A. Such beneficial power of the chemosensor array can determine levels of steroid hormones in metabolism based on the difference in ring A skeletons (*e.g.*, testosterone (H2) and 17β-estradiol (H7)).[1] Therefore, the colorimetric chemosensor array was applied to a semi-quantitative assay of testosterone (H2) and 17β-estradiol (H7) in their mixtures. The LDA canonical score plot (Fig. 4) indicates cluster distribution depending on the molar ratios (H2 : H7) at 100 : 0, 80 : 20, 60 : 40, 40 : 60, 20 : 80, and 0 : 100, which achieved the discrimination of levels of sex hormones with a 100% correct classification rate.

Furthermore, the applicability of the colorimetric chemosensor was evaluated by quantitative assay for salivary markers (*i.e.*, dehydroepiandrosterone (H5), 17β-estradiol (H7), and progesterone (H13)). The employed method, a support vector machine (SVM) allows building a linear calibration line from datasets showing nonlinear sensor responses.[4a,11] The discriminatory power of the chemosensor array for the above salivary markers in their mixtures was revealed by regression analysis with SVM (Fig. S45, ESI†). Thus, we further demonstrated the detection of progesterone (H13) in diluted human saliva samples (ethics authorization code: 24-385). The assay aimed to predict concentrations of progesterone (H13) in the human saliva samples. The predicted datasets (light blue diamonds) were distributed on the calibration line (blue squares) with SVM (Fig. 5), which suggested that the accurate prediction of the target hormone was achieved with low root-mean-square errors for calibration (RMSEC) and prediction (RMSEP) values.

In summary, we designed colorimetric chemosensors for qualitative and quantitative detection of steroid hormones

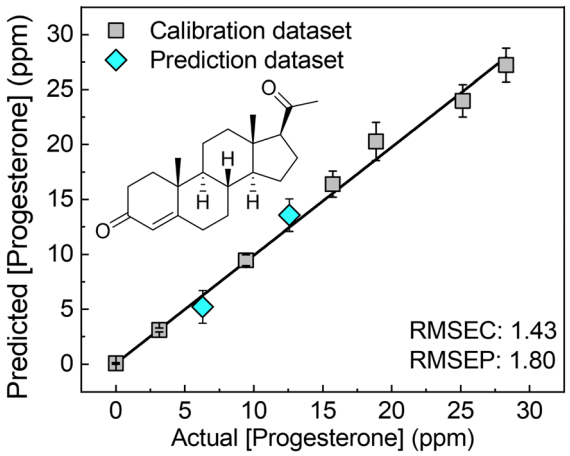

Fig. 5 Regression analysis using SVM for progesterone (H13) in diluted human saliva. RMSEC and RMSEP represent root-mean-square errors for calibration and prediction, respectively.

based on pattern recognition. The chemosensors consisting of indicators (**1**–**3**) and CB[8] showed obvious color changes upon adding the target steroid hormones based on displacement manners. The molecular self-assembled system provided different binding affinities, which suggested the possibility of pattern recognition-driven chemical sensing. The LDA canonical score plot in the qualitative assay showed a high classification rate for 15 steroid hormones. The result indicated the potential of the chemosensor array allowing the cluster categorization based on chemical information including analyte structures and their hydrophilicity. Moreover, the chemosensor array was applied to discriminate levels of testosterone and 17β-estradiol in their mixtures. Each cluster was distributed by changing the molar ratio of the sex hormones with 100% correct classification, which suggested the quantitative discriminatory power of the chemosensor array. Furthermore, the chemosensor array was applied to the quantitative assay for the mixtures of steroid hormones using SVM. The regression analysis results revealed that the self-assembled chemosensor array allowed the detection of the steroid hormone in diluted human saliva. Overall, we first achieved quantitative detection of steroid hormones using the CB[*n*]-based colorimetric chemosensor array, which revealed the potential of machine learning methods for IDA-based quantitative detection of steroid hormones. We believe that the proposed chemosensing approach combined with pattern recognition methods will lead to new analytical tools to not only visualize slight differences in chemical structures and their properties of steroid hormones but also the quantitative detection of steroid hormones in their mixtures and the presence of interferents.

Y. Sasaki gratefully acknowledges the financial support from the Japan Society for the Promotion of Science (JSPS) KAKENHI (Grant No. JP24K17667), JST PRESTO (Grant No. JPMJPR23H2), and Casio Science Promotion Foundation. T. Minami thanks JSPS KAKENHI (Grant No. JP23H03864 and JP24K01315) and JST CREST (Grant No. JPMJCR2011). K. Ohshiro and X. Lyu thanks the JSPS Research Fellow for Young Scientists (DC1) (Grant No. JP23KJ0785 and JP22J23435). The authors greatly thank Mrs Kazuhiko Tsuchiya and Akira Matsumoto for providing beneficial discussions on ^{1}H NMR analysis. The MALDI-TOF MS analysis was carried out using analytical equipment at Komaba Analysis Core, Institute of Industrial Science, The University of Tokyo. The data analysis was carried out with the support of Mr Kohsaku Okuyama.

Data availability

The data supporting this article have been included as part of the ESI.†

Conflicts of interest

There are no conflicts of interest to declare.

References

1 Reviews for steroid hormones, see: (*a*) G. Rastrelli, G. Corona and M. Maggi, *Maturitas*, 2018, **112**, 46–52; (*b*) N. Russell and M. Grossmann, *Eur. J. Endocrinol.*, 2019, **181**, R23–R43; (*c*) E. Olesti, J. Boccard, G. Visconti, V. González-Ruiz and S. Rudaz, *J. Steroid Biochem. Mol. Biol.*, 2021, **206**, 105797; (*d*) H. Kim, Y. Kim, J. Chang, J. Ko and H. Kho, *Oral Diseases*, 2012, **18**, 613–620.
2 (*a*) A. D. Gill, L. Perez, I. N. Q. Salinas, S. R. Byers, Y. Liu, B. L. Hickey, W. Zhong and R. J. Hooley, *Chem. – Eur. J.*, 2019, **25**, 1740–1745; (*b*) M. Yamashina, T. Tsutsui, Y. Sei, M. Akita and M. Yoshizawa, *Sci. Adv.*, 2019, **5**, eaav3179.
3 Reviews for steroid detection using CB[n]s, see: (*a*) L. Isaacs, *Acc. Chem. Res.*, 2014, **47**, 2052–2062; (*b*) Q. Duan, R. Chen, S. Deng, C. Yang, X. Ji, G. Qi, H. Li, X. Li, S. Chen, M. Lou and K. Lu, *Front. Chem.*, 2023, **11**, 1124705. Examples, see: (*c*) D. Ma, B. Zhang, U. Hoffmann, M. Grosse-Sundrup, M. Eikermann and L. Isaacs, *Angew. Chem., Int. Ed.*, 2012, **51**, 11358–11362; (*d*) A. I. Lazar, F. Biedermann, K. R. Mustafina, K. I. Assaf, A. Hennig and W. M. Nau, *J. Am. Chem. Soc.*, 2016, **138**, 13022–13029.
4 (*a*) T. Minami, N. A. Esipenko, B. Zhang, M. E. Kozelkova, L. Isaacs, R. Nishiyabu, Y. Kubo and P. Anzenbacher, Jr., *J. Am. Chem. Soc.*, 2012, **134**, 20021–20024; (*b*) T. Minami, N. A. Esipenko, B. Zhang, L. Isaacs and P. Anzenbacher Jr., *Chem. Commun.*, 2014, **50**, 61–63; (*c*) S. Shradha, R. Kommidi and B. D. Smith, *J. Org. Chem.*, 2023, **88**, 8431–8440.
5 B. Wang and E. V. Anslyn, *Chemosensors: Principles, Strategies, and Applications*, Wiley, Hoboken, 2011.
6 Reviews for cross-reactive sensors, see: (*a*) A. C. Sedgwick, J. T. Brewster, T. Wu, X. Feng, S. D. Bull, X. Qian, J. L. Sessler, T. D. James, E. V. Anslyn and X. Sun, *Chem. Soc. Rev.*, 2021, **50**, 9–38; (*b*) Y. Sasaki, R. Kubota and T. Minami, *Coord. Chem. Rev.*, 2021, **429**, 213607. Examples, see: (*c*) Y. Sasaki, S. Kojima, V. Hamedpour, R. Kubota, S. Takizawa, I. Yoshikawa, H. Houjou, Y. Kubo and T. Minami, *Chem. Sci.*, 2020, **11**, 3790–3796; (*d*) X. Yao and M. Bonizzoni, *Anal. Sens.*, 2023, **3**, e202200057.
7 (*a*) S. Stoyanov, L. Antonov, T. Stoyanova and V. Petrova, *Dyes Pigm.*, 1996, **32**, 171–185; (*b*) L. Antonov, K. Kamada, D. Nedeltcheva, K. Ohta and F. S. Kamounah, *J. Photochem. Photobiol., A*, 2006, **181**, 274–282.
8 S. M. Martin, Z. J. Knepp, I.-A. Thongchai, K. Englehart, K. Sorto, A. Jaffer, L. A. Fredin and E. R. Young, *New J. Chem.*, 2023, **47**, 11882–11889.
9 J. N. Miller and J. C. Miller, *Statistics and Chemometrics for Analytical Chemistry*, Pearson Prentice Hall, Essex, 2005.
10 (*a*) P. Anzenbacher, Jr., P. Lubal, P. Buček, M. A. Palacios and M. E. Kozelkova, *Chem. Soc. Rev.*, 2010, **39**, 3954–3979; (*b*) Z. Li, J. R. Askim and K. S. Suslick, *Chem. Rev.*, 2019, **119**, 231–292.
11 L. Hamel, *Knowledge Discovery with Support Vector Machines*, Wiley, New Jersey, 2009.